



Diels-Alder in Aqueous Molecular Hosts: Unusual Regioselectivity and Efficient Catalysis

Michito Yoshizawa, *et al.*
Science **312**, 251 (2006);
DOI: 10.1126/science.1124985

The following resources related to this article are available online at www.sciencemag.org (this information is current as of July 30, 2007):

A correction has been published for this article at:
<http://www.sciencemag.org/cgi/content/full/312/5779/1472b>

Updated information and services, including high-resolution figures, can be found in the online version of this article at:
<http://www.sciencemag.org/cgi/content/full/312/5771/251>

Supporting Online Material can be found at:
<http://www.sciencemag.org/cgi/content/full/312/5771/251/DC1>

A list of selected additional articles on the Science Web sites **related to this article** can be found at:
<http://www.sciencemag.org/cgi/content/full/312/5771/251#related-content>

This article has been **cited by** 22 article(s) on the ISI Web of Science.

This article has been **cited by** 1 articles hosted by HighWire Press; see:
<http://www.sciencemag.org/cgi/content/full/312/5771/251#otherarticles>

This article appears in the following **subject collections**:
Chemistry
<http://www.sciencemag.org/cgi/collection/chemistry>

Information about obtaining **reprints** of this article or about obtaining **permission to reproduce this article** in whole or in part can be found at:
<http://www.sciencemag.org/about/permissions.dtl>

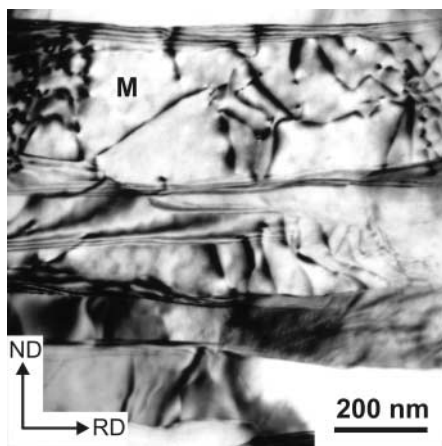


Fig. 4. TEM image showing the lamellar structural morphology and dislocation configuration in the ARB sample processed by annealing at 150°C for 30 min, then deformed 15% by cold rolling. A dislocation structure similar to that in the original ARB sample (Fig. 2A) is introduced in the lamellae.

crease in the elongation by a low level of deformation, are obtained, as shown by curves 4 and 5 in Fig. 3. This repeated mechanical behavior, combined with the structural characterization, confirms that the removal of dislocations by annealing and their introduction by slight deformation are the cause of the changes in the mechanical properties. The deformation induced relatively small decreases in yield stress and UTS, and a large increase in the elongation greatly improves the applicability of the material. A further test of the beneficial effect of deformation as a final processing step is to deform the initial ARB sample 15% by cold rolling. The reason is that this sample has been

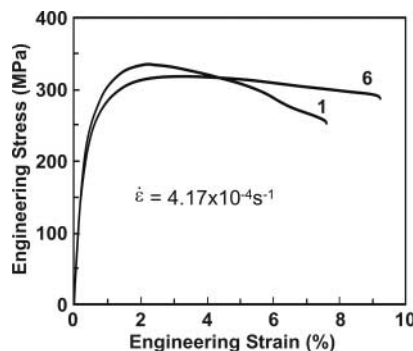


Fig. 5. Engineering stress-strain curves for 99.2% pure Al. Curve 1: same as curve 1 in Fig. 1. Curve 6: same as 1 but deformed 15% by cold rolling. Refer to table S2 for sample numbering.

processed by rolling to a large strain per pass and some adiabatic heating may have taken place (i.e., the material may be in a recovered state) (20). Such conditions are also typical of industrial processing. In accordance with the present hypothesis, it is assumed that a light deformation of an ARB sample in the as-delivered state may induce a small decrease in strength followed by an increase in ductility. Curves 1 and 6 in Fig. 5 confirm this assumption.

The present investigation has focused on aluminum. The strategy described above may also apply to metals such as nickel and interstitial free steels that develop deformation microstructure similar to that of aluminum (14, 21). Therefore, this strategy opens up a research area of both fundamental and applied importance.

References and Notes

1. Y. Wang, M. W. Chen, F. H. Zhou, E. Ma, *Nature* **419**, 912 (2002).

2. G. E. Fougere, J. R. Weertman, R. W. Siegel, S. Kim, *Scr. Metall. Mater.* **26**, 1879 (1992).
3. J. R. Weertman, P. G. Sanders, *Solid State Phenom.* **35–36**, 249 (1994).
4. J. R. Weertman, *Mater. Sci. Eng. A* **166**, 161 (1993).
5. Y. M. Wang *et al.*, *Scr. Mater.* **51**, 1023 (2004).
6. F. Ebrahimi, Q. Zhai, D. Kong, *Scr. Mater.* **39**, 315 (1998).
7. R. Z. Valiev, F. Chmelik, F. Bordeau, G. Kapelski, B. Baudelet, *Scr. Metall. Mater.* **27**, 855 (1992).
8. J. Langoullume *et al.*, *Acta Metall. Mater.* **41**, 2953 (1993).
9. N. Kamikawa, thesis, Osaka University (2005).
10. J. R. Bowen, P. B. Prangnell, D. Juul Jensen, N. Hansen, *Mater. Sci. Eng. A* **387–389**, 235 (2004).
11. A. Hasnaoui, H. V. Swygenhoven, P. M. Derlet, *Acta Mater.* **50**, 3927 (2002).
12. N. Tsuji, Y. Saito, S. H. Lee, Y. Minamino, *Adv. Eng. Mater.* **5**, 338 (2003).
13. See supporting material on Science Online.
14. D. A. Hughes, N. Hansen, *Acta Mater.* **48**, 2985 (2000).
15. Q. Liu, X. Huang, D. J. Lloyd, N. Hansen, *Acta Mater.* **50**, 3789 (2002).
16. E. O. Hall, *Proc. Phys. Soc. London* **B64**, 747 (1951).
17. N. J. Petch, *J. Iron Steel Inst. London* **174**, 25 (1953).
18. J. R. Greer, C. O. Warren, W. D. Nix, *Acta Mater.* **53**, 1821 (2005).
19. J. Schiøtz, K. W. Jacobsen, *Science* **301**, 1357 (2003).
20. N. Tsuji *et al.*, *Mater. Sci. Eng. A* **350**, 108 (2003).
21. B. L. Li, A. Godfrey, Q. C. Meng, Q. Liu, N. Hansen, *Acta Mater.* **52**, 1069 (2004).
22. Supported by the Danish National Research Foundation through the Center for Fundamental Research: Metal Structures in Four Dimensions, within which this work was performed, and by the 21st Century COE Program (the Center of Excellence for Advanced Structural and Functional Materials Design) at Osaka University through MEXT Japan. We thank D. Juul Jensen, B. Ralph, and J. A. Wert for critical reading of the manuscript and helpful discussions; E. Johnson for help with HRTEM; and N. Kamikawa for preparing the samples used in this study.

Supporting Online Material

www.sciencemag.org/cgi/content/full/312/5771/249/DC1
Materials and Methods
Tables S1 and S2
References

23 December 2005; accepted 16 March 2006
10.1126/science.1124268

Diels-Alder in Aqueous Molecular Hosts: Unusual Regioselectivity and Efficient Catalysis

Michito Yoshizawa, Masazumi Tamura, Makoto Fujita*

Self-assembled, hollow molecular structures are appealing as synthetic hosts for mediating chemical reactions. However, product binding has inhibited catalytic turnover in such systems, and selectivity has rarely approached the levels observed in more structurally elaborate natural enzymes. We found that an aqueous organopalladium cage induces highly unusual regioselectivity in the Diels-Alder coupling of anthracene and phthalimide guests, promoting reaction at a terminal rather than central anthracene ring. Moreover, a similar bowl-shaped host attains efficient catalytic turnover in coupling the same substrates (although with the conventional regiochemistry), most likely because the product geometry inhibits the aromatic stacking interactions that attract the planar reagents to the host.

Effective synthetic homogeneous catalysts have generally been structurally simple small molecules, which act by binding to substrates at or near the reaction site. In contrast, enzymes are much larger and

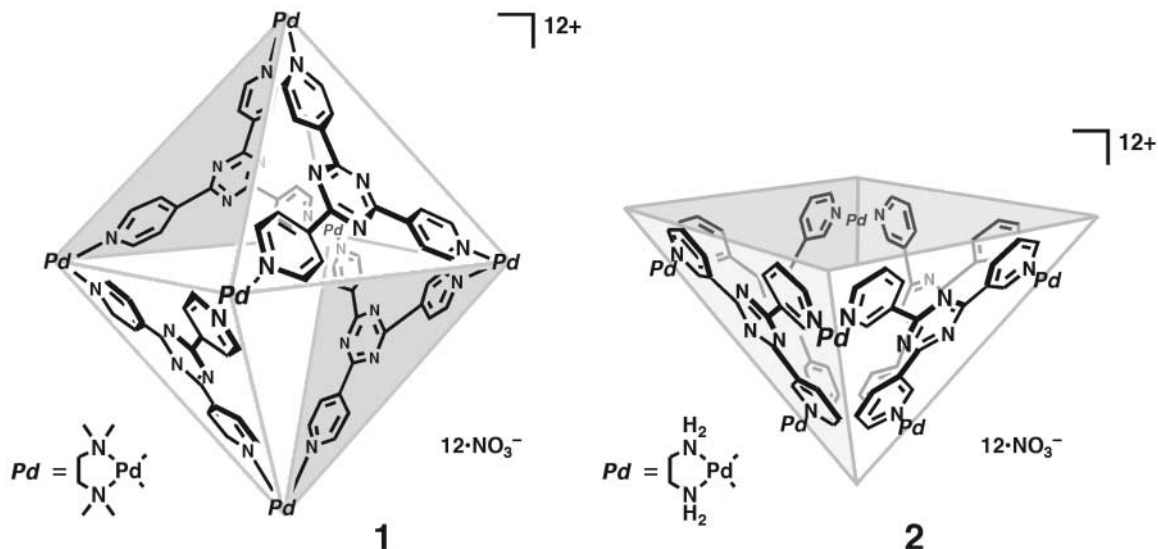
more complex and derive much of their selectivity by bonding substrates through multiple interactions in elaborate pockets, thereby forcing the substrates into orientations that favor specific reaction paths (1, 2). In the past decade, chemists

have made substantial progress in building molecular hosts that emulate these enzymatic pockets (3, 4). Self-assembly of carefully constructed organic and/or metallic building blocks in solution produces hollow host structures that can bind small molecule guests (5, 6). Among the many potential advantages of this strategy is the creation of hydrophobic reaction environments in aqueous solution, widening the scope of accessible reactivity in ecologically friendly media. However, these synthetic hosts have rarely conferred the orientational precision necessary to guide reactions along otherwise unfavored pathways. Moreover, catalytic turnover has been inhibited because the hosts bind products as effectively as reactants, if not more so. In earlier reports by Rebek (7, 8), Sanders (9), and our

Department of Applied Chemistry, School of Engineering, University of Tokyo, and Core Research for Evolutional Science and Technology (CREST), Japan Science and Technology Agency (JST), 7-3-1 Hongo, Bunkyo-ku, Tokyo 113-8656, Japan.

*To whom correspondence should be addressed. E-mail: mfujita@appchem.t.u-tokyo.ac.jp

Fig. 1. Self-assembled coordination cages (**1** and **2**), which are prepared by simple mixing of an exo-tridentate organic ligand and an end-capped Pd(II) ion in a 4:6 ratio in water.



group (10), the Diels-Alder and related cyclo-additions are significantly accelerated in synthetic pockets, but the product inhibition prevents the reactions from showing turnover and the stereochemical courses are not well controlled by the pockets. For catalytic reactions by self-assembled hosts, there have appeared only a few examples, including the Diels-Alder (11), epoxidation (12), and the aza-Cope rearrangement (13). Controlling reaction pathways by encapsulation has been discussed in the excited-state chemistry of aromatic guests (14) and also realized by a regioselective cycloaddition (8).

We investigated the host-mediated Diels-Alder coupling of anthracenes and phthalimides. The Diels-Alder reaction of anthracenes in the absence of hosts is extremely well studied and generally yields an adduct bridging the center ring (9,10-position) of the anthracene framework (15–17) as a consequence of the high localization of π -electron density at that site (18, 19). We find that an appropriately designed cage structure can alter this well-established selectivity to favor adduct formation at a terminal ring (1,4-position). This unusual regioselectivity likely stems from topochemical control induced by the proximity of the 1,4-position of the anthracene to the dienophile in the cage. The 1,4-selective Diels-Alder of anthracenes has been previously reported only for a benzyne addition (20) and for the addition with 9,10-diarylanthracenes (21). We further find that the same reaction, through conventional regioselectivity, can be catalyzed with efficient turnover by a related, bowl-shaped host. As in enzymatic reactions (2, 22), the product geometry, bent at the 9,10-position, precludes the aromatic stacking interactions that underlie the host's affinity for the reagents.

The coordination hosts we used here are octahedral cage **1** and square-pyramidal bowl **2** (Fig. 1) (23–25). Both of them assemble from cis end-capped Pd(II) ions and triazine-cored tridentate ligands in a surprisingly efficient manner (100°C, <5 min, quantitative yields). In

Fig. 2. (A) Pair-selective encapsulation of two types of reactants, 9-hydroxymethylanthracene (**3a**) and *N*-cyclohexylphthalimide (**4a**), within cage **1** and the subsequent Diels-Alder reaction leading to syn isomer of 1,4-adduct **5** within the cavity of **1**. (B) Syn-1,4-regioselective Diels-Alder products within cage **1**. The structures of the adducts and the yields are shown.

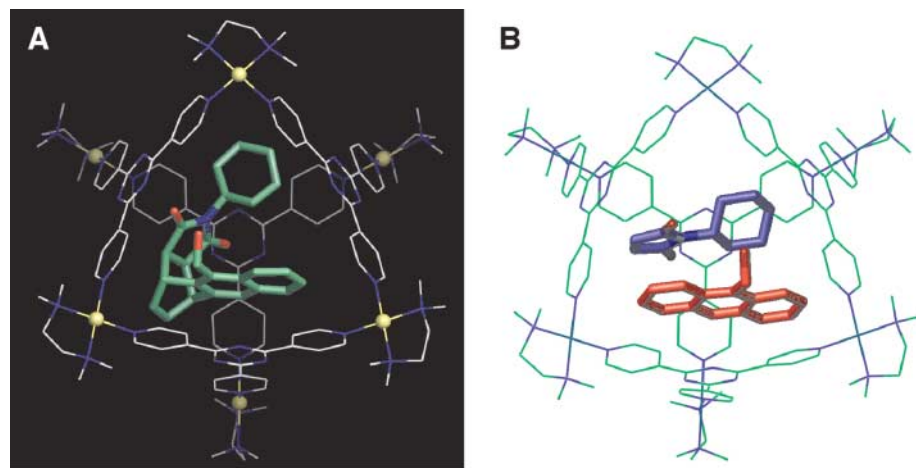
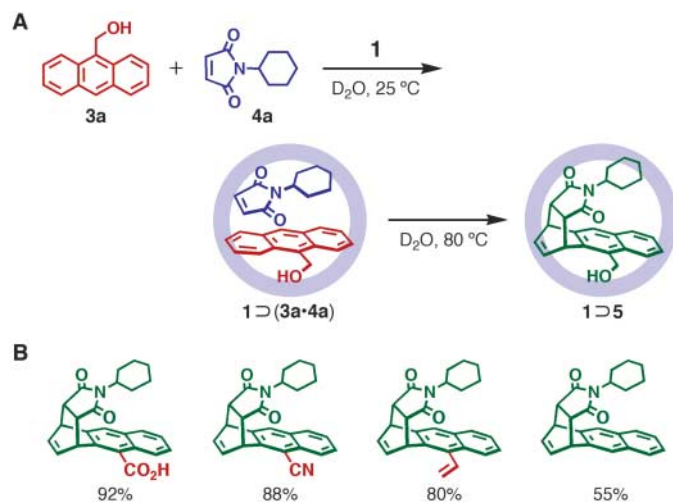


Fig. 3. (A) Crystal structure of **1** \supset **5** and (B) optimized structure (A) of **1** \supset (**3a**·**4a**) by a force-field calculation.

aqueous solution, these structures provide an efficient hydrophobic pocket capable of binding a variety of neutral organic compounds. Cage **1**

features a three-dimensionally enclosed cavity, which binds substrates in precisely fixed positions. Geometry-fixed encapsulation (26), iso-

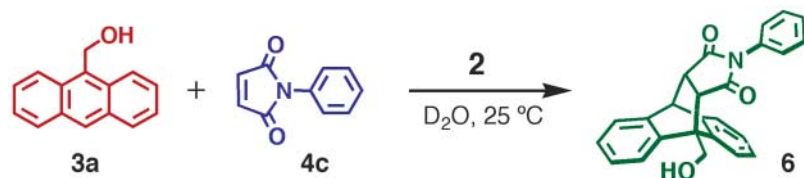


Fig. 4. Catalytic Diels-Alder reaction of 9-hydroxymethylanthracene (**3a**) and *N*-phenylphthalimide (**4c**) in the aqueous solution of bowl **2**, leading to 9,10-adduct **6**.

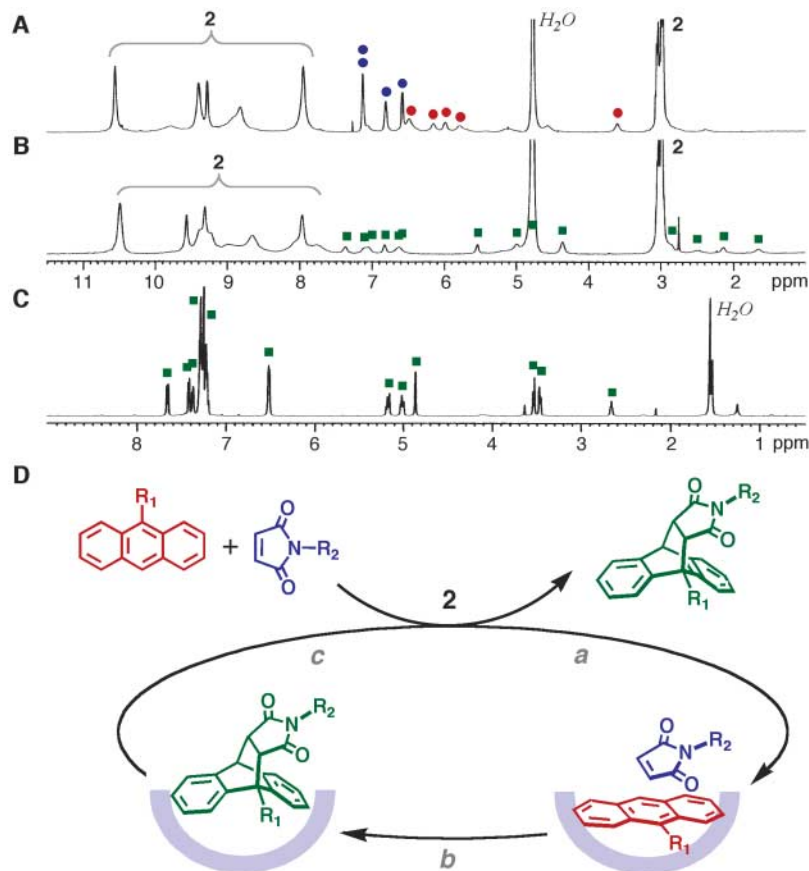


Fig. 5. The ^1H NMR spectra (500 MHz, room temperature) of the catalytic Diels-Alder reaction of 9-hydroxymethylanthracene (**3a**) and *N*-phenylphthalimide (**4c**) in an aqueous solution of bowl **2**. (A) Before and (B) after the reaction at room temperature for 5 hours (red circles, **3a**; blue circles, **4c**; and green squares, **6**). (C) Diels-Alder product **6** after extraction with CDCl_3 . (D) Schematic representation of the catalytic Diels-Alder reaction of anthracenes and phthalimide in the presence of bowl **2**. Autoinclusion of substrates into **2** (step a) and autoexclusion of the product from **2** (step c) underlie the efficient catalytic Diels-Alder reaction.

mer separation (27), pairwise selective inclusion of two guests (28), and stereocontrolled cyclic siloxane formation (29) have been reported. Bowl **2** has an open cavity that facilitates rapid binding and dissociation of substrates (25).

When 9-hydroxymethylanthracene (**3a**) and *N*-cyclohexylphthalimide (**4a**) (6.0 mM) were suspended in an aqueous solution of cage **1** (5.0 mM) at room temperature, the inclusion complex **1** \supset (**3a**•**4a**) (this set notation denotes that **1** includes **3a** and **4a**) formed selectively within 5 min (Fig. 2A). A ^1H nuclear magnetic resonance (NMR) analysis confirmed the encapsulation, with the resonances of **3a** and **4a**

shifted far upfield because of interaction with the cage (fig. S1a) (30). No signals indicating **1** \supset (**3a**)_{*n*} or **1** \supset (**4a**)_{*n*} (*n* ≤ 2) were observed in the NMR spectrum. On heating the solution at 80°C for 5 hours, the signals derived from **3a** and **4a** disappeared and were replaced by resonances consistent with a Diels-Alder adduct, distributed between 6.8 and -2.1 parts per million (ppm) (fig. S1b). Sixteen signals in the 9.7- to 8.4-ppm range were observed for cage **1**, indicating the desymmetrization of the cage from T_d to C_3 symmetry (26). This symmetry agreed with the restricted motion of a noncentrosymmetric product along the C_3 axis, which is per-

pendicular to one of the triazine ligands (**30**). After insoluble solids were removed by filtration, the product was extracted into CDCl_3 and fully assigned as the syn isomer of 1,4-Diels-Alder adduct **5** (fig. S4). No other regio- or stereoisomers (1,9-adduct or anti-1,4-adduct) were detected. The yield of **5** was estimated to be >98% (based on **1**) from the ^1H NMR spectra (30). In contrast, in the absence of **1**, the reaction gave only the conventional 9,10-Diels-Alder adduct in 44% yield based on **3a**.

The unusual structure of the 1,4-Diels-Alder adduct was unambiguously determined by x-ray crystallographic analysis of **1** \supset **5** (Fig. 3A). A single crystal suitable for x-ray analysis was obtained by the slow evaporation of water from an aqueous solution of **1** \supset **5** over 5 days (30). The crystal structure displays the syn stereochemistry of 1,4-adduct **5**, which is tightly accommodated in the cavity of **1** via π - π stacking interactions (3.3 Å) between the naphthalene ring of **5** and a triazine ligand of **1**.

Because the Diels-Alder reaction has an early transition state (15), the unusual regio- and stereoselectivities can be explained by the fixed orientation of the guests before the reaction. The geometries of **3a** and **4a** in the **1** \supset (**3a**•**4a**) complex were modeled by force-field calculation (31). Randomly oriented **3a** and **4a** guests in several initial structures converged in all cases to a parallel orientation with the C=C bond of **4a** in close contact with the 1,4-position of **3a** (Fig. 3B). The center-to-center distance between the two reaction centers is only circa (ca.) 3.8 Å, which is comparable to the sum of van der Waals radii. Because of the steric restrictions induced by the cage, the C=C bond of **4a** hardly interacts with the 9,10-position of **3a** (ca. 4.7 Å). It is also interesting that the cavity of **1** directs exo-selective addition of **4a** to the 1,3-diene moiety of **3a**, yielding only exo-selective syn adduct **5**.

The 1,4-regioselective Diels-Alder reaction also proceeded with varied substrates. Carboxyl-, cyano-, and vinyl-substituted anthracenes coupled with phthalimide **4a** to give the corresponding 1,4-adducts in 92, 88, and 80% yields, respectively (Fig. 2B) (30). Unsubstituted anthracene also afforded only the 1,4-adduct in 55% yield. The moderate yield for this substrate is due not to reduced regio- or stereoselectivity but to the less efficient inclusion process before the reaction. The steric bulkiness of the *N*-substituent on the dienophile is crucial to the 1,4-selectivity. When sterically less demanding *N*-propylphthalimide (**4b**) was used, only the 9,10-adduct was formed.

We turned next to investigating Diels-Alder mediation by bowl-shaped host **2** and, strikingly, observed efficient catalytic turnover. Only 10 mole percent (mol %) of **2** sufficed to catalyze the Diels-Alder reaction of **3a** and *N*-phenylphthalimide (**4c**) (Fig. 4). When **3a** (10.0 μmol) and *N*-phenylphthalimide (**4c**, 10.0 μmol) were suspended in an aque-

ous solution of **2** (1.0 μmol in 1.0 ml) at room temperature for 5 hours (Fig. 5, A and B), the Diels-Alder adduct formed quantitatively (>99% based on **3a**), as evaluated by NMR analysis of the product (**32**). NMR analysis also indicated that the reaction took place at the normal 9,10-position of anthracene to give **6** (Fig. 5C). In the absence of bowl **2**, the reaction hardly proceeded (only 3% yield) under the same conditions. Surprisingly, even in the presence of 1 mol % of **2**, adduct **3a** was obtained in >99% yield after 1 day as estimated by the NMR spectrum in CDCl_3 . Moreover, the metal component, (en)Pd(NO₃)₂ (where en is ethylenediamine) alone, did not catalyze the reaction (**30**). Therefore, the data support promotion of the reaction by the hydrophobic pocket of **2**.

Bowl **2** also efficiently catalyzed Diels-Alder coupling of a variety of anthracene and phthalimide derivatives (**30**). When **3a** and *N*-propyl- or *N*-benzylphthalimide were suspended in an aqueous solution of **2**, the corresponding Diels-Alder products were obtained in almost quantitative yields after 5 hours at room temperature. In addition, 9-methyl and 9-vinylnanthracene reacted with **4c** in the presence of a catalytic amount of **2** (10 mol %).

Product inhibition has been a serious problem in previous examples of cavity-promoted Diels-Alder reactions with synthetic hosts (**7–11**). Because of the entropic disadvantage arising from the need to bind two reactant molecules, the encapsulated product has generally been a thermodynamic sink. Therefore, the reactions require near-stoichiometric quantities of host. It is noteworthy that, in contrast to previous examples, the present Diels-Alder reaction involves an exclusion step in the catalytic cycle. Before the reaction, anthracene can stack onto the triazine ligand of **2**, gaining considerable stabilization via aromatic-

aromatic or charge-transfer interactions (Fig. 5D, step a). The reactant-like transition state is similarly stabilized. However, once the reaction is complete, the product framework is bent at the 9,10-position, cutting off the host-guest aromatic stacking interaction (Fig. 5D, step b). Accordingly, the encapsulated product is considerably destabilized and smoothly replaced by incoming reagents (Fig. 5D, step c \rightarrow a). In this sense, the affinity of the host for reactive substrates and the disaffinity for product is markedly similar to enzymatic behavior.

References and Notes

1. L. Pauling, *Am. Sci.* **36**, 51 (1948).
2. W. P. Jencks, *Catalysis in Chemistry and Enzymology* (McGraw-Hill, New York, 1969).
3. D. J. Cram, J. M. Cram, *Container Molecules and Their Guests* (Royal Society of Chemistry, Cambridge, 1994).
4. J. W. Steed, J. L. Atwood, *Supramolecular Chemistry* (Wiley, Chichester, UK, 2000).
5. F. Hof, S. L. Craig, C. Nuckolls, J. Rebek Jr., *Angew. Chem. Int. Ed. Engl.* **41**, 1488 (2002).
6. D. M. Vriezema *et al.*, *Chem. Rev.* **105**, 1445 (2005).
7. J. Kang, J. Rebek Jr., *Nature* **385**, 50 (1997).
8. J. Chen, J. Rebek Jr., *Org. Lett.* **4**, 327 (2002).
9. M. Marty, Z. C.-Watson, L. J. Twyman, M. Nakash, J. K. M. Sanders, *Chem. Commun.* **1998**, 2265 (1998).
10. T. Kusakawa, T. Nakai, T. Okano, M. Fujita, *Chem. Lett.* **32**, 284 (2003).
11. J. Kang, J. Santamaria, G. Hilmersson, J. Rebek Jr., *J. Am. Chem. Soc.* **120**, 7389 (1998).
12. M. L. Merlau, M. P. Mejia, S. T. Nguyen, J. T. Hupp, *Angew. Chem. Int. Ed. Engl.* **40**, 4239 (2001).
13. D. Fiedler, R. G. Bergman, K. N. Raymond, *Angew. Chem. Int. Ed. Engl.* **43**, 6748 (2004).
14. L. S. Kaanumalle, C. L. D. Gibb, B. C. Gibb, V. Ramamurthy, *J. Am. Chem. Soc.* **127**, 3674 (2005).
15. F. Fringuelli, A. Taticchi, *The Diels-Alder Reaction: Selected Practical Methods* (Wiley, Chichester, UK, 2002).
16. R. Breslow, *Acc. Chem. Res.* **24**, 159 (1991).
17. F. Stuhlmann, A. Jäschke, *J. Am. Chem. Soc.* **124**, 3238 (2002).
18. M.-F. Cheng, W.-K. Li, *Chem. Phys. Lett.* **368**, 630 (2003).
19. Computational study [MP2(FULL)/6-31G(d) level] of the Diels-Alder reactions of anthracene and ethylene indicates that the reaction barrier to formation of the 1,4-adduct is much higher than that characterizing the 9,10-adduct ($\Delta E = 29.6$ kJ/mol).
20. B. H. Klanderman, *J. Am. Chem. Soc.* **87**, 4649 (1965).
21. J. Rigaudy, P. Scribe, C. Brelie, *Tetrahedron* **37**, 2585 (1981).
22. T. Ose *et al.*, *Nature* **422**, 185 (2003).
23. M. Fujita *et al.*, *Nature* **378**, 469 (1995).
24. Coordination cages (**1** and **2**) are now commercially available from Wako Pure Chemicals Industries Limited, Osaka, Japan (Pd-Nanocage and Pd-Nanobowl, respectively). Cage **1** is an analog of **1** in which ethylenediamine on the Pd(II) ions is replaced by *N,N,N',N'*-tetramethylethylenediamine.
25. S.-Y. Yu, T. Kusakawa, K. Biradha, M. Fujita, *J. Am. Chem. Soc.* **122**, 2665 (2000).
26. T. Kusakawa, M. Yoshizawa, M. Fujita, *Angew. Chem. Int. Ed. Engl.* **40**, 1879 (2001).
27. T. Kusakawa, M. Fujita, *J. Am. Chem. Soc.* **121**, 1397 (1999).
28. M. Yoshizawa, M. Tamura, M. Fujita, *J. Am. Chem. Soc.* **126**, 6846 (2004).
29. M. Yoshizawa, T. Kusakawa, S. Sakamoto, K. Yamaguchi, M. Fujita, *J. Am. Chem. Soc.* **123**, 10454 (2001).
30. See Materials and Methods available at Science Online. Metrical data for the crystal structure of **1** \supset **5** are available free of charge from the Cambridge Crystallographic Data Centre under reference CCDC-293777.
31. Force-field calculations were carried out with the use of the Cerius² 3.5 software package (Molecular Simulation Incorporated, San Diego, CA, 1997).
32. Because no decomposition or side products were observed in the NMR spectra of the reactions catalyzed by **2** either during reaction in D₂O or after extraction into CDCl₃, the reported NMR yields have their basis in the product purity observed in the spectra of the CDCl₃ extract.
33. This work was financially supported by a Grant-in-Aid for Scientific Research (S), no. 14103014, from the Ministry of Education, Culture, Sports, Science, and Technology of Japan.

Supporting Online Material

www.sciencemag.org/cgi/content/full/312/5771/251/DC1
Materials and Methods
Figs. S1 to S18
Tables S1 and S2

17 January 2006; accepted 13 March 2006
10.1126/science.1124985

Double Perovskites as Anode Materials for Solid-Oxide Fuel Cells

Yun-Hui Huang, Ronald I. Dass, Zheng-Liang Xing, John B. Goodenough*

Extensive efforts to develop a solid-oxide fuel cell for transportation, the bottoming cycle of a power plant, and distributed generation of electric energy are motivated by a need for greater fuel efficiency and reduced air pollution. Barriers to the introduction of hydrogen as the fuel have stimulated interest in developing an anode material that can be used with natural gas under operating temperatures $650^\circ\text{C} < T < 1000^\circ\text{C}$. Here we report identification of the double perovskites $\text{Sr}_2\text{Mg}_{1-x}\text{Mn}_x\text{MoO}_{6-\delta}$ that meet the requirements for long-term stability with tolerance to sulfur and show a superior single-cell performance in hydrogen and methane.

Development of an anode material for a solid-oxide fuel cell (SOFC) that operates on natural gas is widely recognized to be an important technical objective (**1–6**). The conventional NiO/electrolyte composite anode gives good performance with pure H₂ as fuel. The H₂ fuel reduces the NiO to

elemental nickel, which leaves a porous oxide-ion electrolyte in which the walls of the pores are coated with Ni⁰ particles that not only catalyze breaking of the H₂ bond but also provide electronic conduction from the reaction site to the current collector. However, with natural gas, nickel is fouled by carbon deposition (**7**)

unless a large amount of steam is added to the fuel (**8**), and it has a low tolerance to sulfur due to the formation of NiS, which requires a high-grade desulfurization for the fuel (**9**).

Early attempts to identify an alternative anode material consisted of doping transition-metal ions into zirconia (**10**, **11**) or a rare-earth into ceria (**12**). Even where the doped ceria was fabricated as a porous structure with inactive copper on the pore surfaces to provide electronic conduction or with a Y_xCe_{1-x}O_{2-0.5x} buffer layer to improve the electrode/electrolyte bonding, preliminary studies of the catalytic activity of the anode suggest that it remains too low (**13**). However, the ceria-based anode was reported to be effective in preventing carbon formation (**14**) and also to have good tolerance to sulfur (**15**).

Texas Materials Institute, ETC 9.102, The University of Texas at Austin, Austin, TX 78712, USA.

*To whom correspondence should be addressed. E-mail: jgoodenough@mail.utexas.edu

ERRATUM

Post date 9 June 2006

Reports: "Diels-Alder in aqueous molecular hosts: unusual regioselectivity and efficient catalysis" by M. Yoshizawa *et al.* (14 Apr. 2006, p. 251). Due to a nomenclature error, all references to "phthalimides" in the text and Supporting Online Material should instead refer to "maleimides." The chemical structures in the schemes and figures are all correct as drawn.